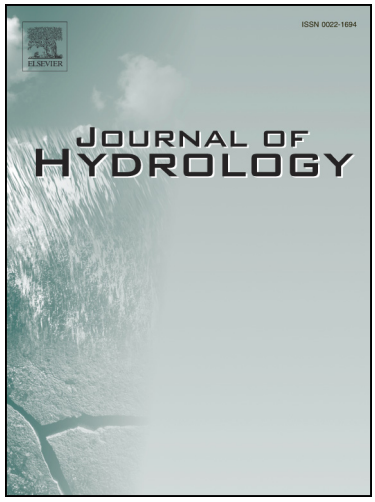

Research papers

Uncertainty of groundwater recharge estimated from a water and energy balance model

Yueqing Xie, Peter G. Cook, Craig T. Simmons, Daniel Partington, Russell Crosbie, Okke Batelaan

PII: S0022-1694(17)30536-X
DOI: http://dx.doi.org/10.1016/j.jhydrol.2017.08.010
Reference: HYDROL 22173

To appear in: *Journal of Hydrology*

Please cite this article as: Xie, Y., Cook, P.G., Simmons, C.T., Partington, D., Crosbie, R., Batelaan, O., Uncertainty of groundwater recharge estimated from a water and energy balance model, *Journal of Hydrology* (2017), doi: http://dx.doi.org/10.1016/j.jhydrol.2017.08.010

Uncertainty of groundwater recharge estimated from a water and energy balance model

Yueqing Xie[1], Peter G. Cook[1], Craig T. Simmons[1], Daniel Partington[1], Russell Crosbie[2], Okke Batelaan[1]

[1] National Centre for Groundwater Research and Training, Colleague of Science and Engineering, Flinders University, Adelaide, South Australia, Australia

[2] CSIRO Land and Water, Adelaide, South Australia, Australia

For submission to Journal of Hydrology

Abstract

Coupled water and energy balance models have become increasingly popular for estimating groundwater recharge, because of the integration of energy and water balances and sometimes carbon balance. The additional balances are thought to constrain the water balance and as a result should help reduce the uncertainty of groundwater recharge. However, these models usually have a large number of parameters. The uncertainty of these parameters may result in a large uncertainty in groundwater recharge estimates. This study aims to assess the potential uncertainty of groundwater recharge estimated from a widely used water and energy model. It is largely based on annual pasture vegetation in the lower part of the Campaspe catchment in southeast Australia. A Monte Carlo analysis method was employed to examine potential uncertainties introduced by different types of errors. The results show that for a mean rainfall of 398 mm/y and using a particular set of pedotransfer functions for deriving soil hydraulic parameters, the estimated recharge ranged from 7 to 144 mm/y due to the uncertainty in vegetation parameters. This upper bound of the recharge range increased to 236 mm/y when using different sets of pedotransfer functions. Through several synthetic test cases, this study shows that soil moisture time series may not offer much help for reducing recharge uncertainty, whereas evapotranspiration time series are able to reduce recharge uncertainty by more than 50%. The reduction in recharge uncertainty steadily improves as the uncertainty in observations reduces.

1. Introduction

Groundwater recharge plays a significant role in water resources management, in particular in arid and semi-arid regions (Scanlon et al., 2006). Often, groundwater recharge is used to determine the allocation of groundwater extraction, based on the principle that the extraction should not exceed the recharge. Although the relationship between allocation and recharge has been criticised (e.g., Bredehoeft, 1997, 2002; Gorelick and Zheng, 2015; Zhou, 2009), the practice is still common throughout the world (e.g., Chung et al., 2016; Devlin and Sophocleous, 2005).

Many methods have been developed to estimate groundwater recharge, with the soil water balance method probably the most widely used and perhaps the most straightforward (Allison et al. 1994; Healy and Cook, 2002; Scanlon et al., 2002). A large number of soil water balance models have been developed, and these can be broadly classified into bucket models and physically based models. The bucket models treat the soil as a reservoir that is filled up by precipitation and emptied by evapotranspiration (Zhang et al., 2002). Recharge occurs when the reservoir overflows. Numerous variants of bucket models exist depending on the conceptualisation of the system and methods for estimating evapotranspiration (Alley, 1984; Dripps and Bradbury, 2007; Finch, 1998; Jie et al., 2011; Kendy et al., 2003; Ruiz et al., 2010; Rushton and Ward, 1979; Westenbroek et al., 2010; Zhang and Hiscock, 2010). These models are computationally efficient and so have been used over large areas (Xu, 1997; Xu and Singh, 1998). In comparison, physically-based soil water balance models have to solve Richards' equation to obtain the spatial distribution of soil moisture content (Chen et al., 2014; Cheng et al., 2014; Kurtzman and Scanlon, 2011; Turkeltaub et al., 2015). The computational burden and the difficulty to achieve numerical convergence restrict physically

based models to be mostly used for assessing local-scale hydrological process and quantifying relevant fluxes.

Water and energy balance models are essentially water balance models capable of simulating the water and energy balances simultaneously (e.g., Akkermans et al., 2012; Petropoulos et al., 2009; Sellers et al. 1986; Williams et al., 1996; Zhang and Dawes 1998). Because of their additional capacity to simulate the energy balance, these models are considered superior to water balance only models for computing evapotranspiration (Overgaard et al. 2006). Potential groundwater recharge, which is the rate of soil water drainage below a given depth, is a water budget component that is produced from all water and energy balance models. The use of water and energy balance models to estimate potential groundwater recharge in Australia started from the need to address the response of potential recharge to land use changes (Zhang et al., 1999) and climate change (Crosbie et al., 2010; McCallum et al., 2010). The WAter Atmosphere Vegetation Energy and Solutes model (WAVES) was the model used (Zhang and Dawes 1998). Since then, the WAVES model has been applied in many areas to assess groundwater recharge (Crosbie et al., 2012, 2013). Models are usually calibrated to different observations, including streamflow, soil moisture, evapotranspiration and MODIS leaf area index (Chen et al., 2014; Cheng et al., 2014; Zhang et al., 1999).

Conceptually, models which are more complex and include a larger number of physical processes should be more accurate than overly simple models that neglect critical processes, although this may depend on the uncertainty associated with calibration data and model parameters. This is because simple models have large structural errors, and estimating parameter values based on soft knowledge is often better than neglecting processes entirely. Water and energy balance models may help to better constrain the water balance with the

energy and carbon balances in comparison to pure water balance models, as these additional balances constrain evapotranspiration (ET). For example, ET is influenced by net radiation, air temperature, vapour pressure deficit, aerodynamic resistance and canopy resistance. Canopy resistance is a function of relative availability of water and light, carbon assimilation rate, leaf area index. Although the accuracy of water balance models for estimating groundwater recharge has been questioned in a number of studies (e.g., Alley, 1984; Gee and Hillel, 1988), there are still very few examples of where formal uncertainty analysis has accompanied estimates of recharge obtained with such models, even for simple models with few parameter values (Giambelluca et al., 1996; Lanini and Caballero, 2016). It is clear that models that are calibrated to field data should also have less uncertainty than uncalibrated models, although calibration data can be difficult to obtain and/or site-specific. Nevertheless, it is not uncommon to predict recharge using models without any formal calibration (e.g., Dash et al, 2016; Crosbie et al., 2010, 2011, 2013; Rushton et al. 2006; Taylor and Howard, 1996).

The objectives of this study were to examine the uncertainty of groundwater recharge estimated from a water and energy balance model that has been widely used around the world and also to provide suggestions for reducing uncertainty when using this type of model. The intention was not to exhaust all the possible scenarios but rather to address this issue through a synthetic example largely based on a field site in southeast Australia. We built a model in a similar manner to that described in Crosbie et al. (2010) to represent typical land use (C3 annual pasture or dryland pasture in this study) in a semi-arid area. A Monte Carlo approach was adopted to examine potential uncertainty using Latin-Hypercube sampling. We then explored whether field observations such as soil moisture and evapotranspiration could be employed to reduce recharge uncertainty.

2. Field site description

This study is loosely based on the lower part of the Campaspe catchment in southeast Australia (**Figure 1**). We chose the annual pasture in this area as our vegetation. The intention of this study was not to produce recharge estimates across the entire region. Rather, we aimed to illustrate potential recharge uncertainty estimated from a water and energy balance model using a demonstrative example.

The northern part of the catchment includes the floodplains of the Campaspe and Murray rivers as so is very flat. The top soil over this region largely falls in the category of Sodosols according to the Australian Soil Classification system (Isbell, 1996). Two aquifers occur in this area: an unconfined sand-clay interbedded aquifer and a semi-confined sandy aquifer. The water table in the unconfined aquifer is generally 10-15m below ground, whereas the piezometric surface in the confined aquifer is lower than the water table. Therefore, there is a general trend of downward flow from the unconfined aquifer to the confined aquifer. The long-term average precipitation is about 400 mm/y, whereas the long-term average potential evapotranspiration (ET) is 1600 mm/y (2006-2016). Rainfall occurs episodically throughout the year, with monthly rainfall about 1/3 higher in the months from May to October (around 40 mm) than in other months. However, extreme rainfall events can occur at any time. In comparison, potential ET has a clear seasonal trend. It peaks at around 12 mm/d in the summer months (December to February) and is around 1 mm/d in the winter months (June to August). The majority of the catchment has been cultivated for farming. Dryland crops, dryland pasture and irrigated crops account for 6%, 69% and 8% of the total catchment area, respectively. This study has focused on dryland pasture (C3 annual pasture which belongs to the plant functional type of grass), as this is the dominant vegetation type in the catchment.

3. Methods

3.1 Numerical modelling

The WAter Atmosphere Vegetation Energy and Solutes (WAVES) model (Zhang and Dawes 1998) was chosen to examine recharge uncertainty estimated from the water and energy balance modelling. WAVES simulates water, solute, energy and carbon balances simultaneously in the soil-vegetation-atmosphere continuum. Rainfall is first intercepted by plant leaves and then evaporated back to the atmosphere. For any time step, WAVES first performs the calculation of the carbon balance in order to derive the canopy carbon assimilation rate. The carbon assimilation rate is then distributed to leaves, stems and roots based on factors such as water availability, respiration rates and leaf mortality rates. Then WAVES carries out the calculation of the energy balance in order to obtain the ET rate through the Penman-Monteith equation. This ET rate is distributed to different depths of the root zone by considering a number of factors such as root carbon mass, soil water matric potential, osmotic potential, root salt sensitivity factor and permanent wilting point. Next, WAVES iteratively solves the Richards equation to achieve numerical convergence. Excess water above ground due to limited infiltration and saturation capacity becomes overland flow. This excess water above ground is removed from the model by default. Excess water draining through the soil continuum will become groundwater recharge. A detailed description of the methodology used by WAVES and its numerical implementation is thoroughly documented by Zhang and Dawes (1998).

3.2 Data collection and analysis

Three types of data were collected for running the WAVES model. These include climate variables on a daily time step, soil attribute data for deriving soil hydraulic parameters and vegetation parameters.

Historical daily climate data was extracted from the gridded climate surfaces provided by the Queensland Department of Natural Resources and Water (Jeffrey et al., 2001). The dataset contains all the common variables measured at a weather station, including rainfall, temperature, solar radiation, pan evaporation, vapour pressure and humidity, for 127 years. The variable vapour pressure deficit was derived from temperature and measured vapour pressure in accordance with Grayson et al. (1998).

Soil hydraulic parameters were derived from soil attribute raster datasets accessed from the Terrestrial Ecosystem Research Network (TERN, http://www.tern.org.au/). The TERN provides a range of Australia-wide soil attributes (e.g., clay content, silt content, sand content) at 6 depth intervals (0 - 0.05 m, 0.05 - 0.15 m, 0.15 – 0.3 m, 0.3 – 0.6 m, 0.6 – 1.0 m and 1.0 – 2.0 m). The top 0.3 m and the depth range of 0.3 – 2.0 m were treated as topsoil and subsoil, respectively. We considered both topsoil and subsoil in order to account for the fact that topsoil is usually more permeable than subsoil because of its richness in organic matters. This treatment rendered the subsurface structure of the WAVES model consistent with previous studies (e.g., Crosbie et al., 2010, 2012). Then we averaged the clay content of both the topsoil and subsoil to create a clay content map. On the map, grid cells with clay content lower than the median value are classified as soil group 1. The remaining grid cells are classified as soil group 2. This resulted in a soil group map as shown in Figure 1. We used clay content to determine soil groups, as increases in clay content lead to decreases in

permeability and increases in water holding capacity and hence increases in deep drainage (Kennett-Smith et al., 1994; Wohling et al., 2012). The second soil group was chosen to examine the uncertainty of recharge.

The soil attribute values were used to calculate the soil moisture characteristic curves at discrete points through pedotransfer functions. Ideally, a specific pedotransfer function should be derived from field measurements for the study area. However, this was not possible due to the size of the catchment and paucity of data. Minasny et al. (1999) derived a pedotransfer function for Australia but this function was not useful in this study because it requires soil particle size data, which was not available for the field site. Moreover, most studies only have pedotransfer functions for either soil moisture characteristic curves or saturated hydraulic conductivity instead of both. Ultimately, four sets of pedotransfer functions that are capable of deriving both soil moisture characteristic curves and saturated hydraulic conductivity parameters from the same soil data were selected from the literature (i.e., Dane and Puckett, 1992; Saxton et al., 1986; Wösten et al., 1999; Schaap et al., 2001).

As WAVES uses the Broadbridge-White soil retention model (Broadbridge and White, 1998), we derived retention curve parameters and saturated hydraulic conductivity from the four sets of pedotransfer functions (Table 1) for both topsoil and subsoil. It is clear that all the parameters except C are very different from one group to another, indicating the difference between the pedotransfer functions. All the pedotransfer functions yielded C fixed at 10 because this parameter relates to the slope of the moisture characteristic at satiation.

In this study, we chose C3 annual pasture as the vegetation because it is the dominant vegetation type in the catchment. WAVES requires 26 parameters for a type of vegetation.

Dawes and Zhang (1998) conducted a comprehensive literature review of vegetation parameters and compiled a table of all parameters with upper and lower bounds for several different vegetation types. These uncertainties reflect the accuracy of estimation without field measurement. When using a biophysically based model at the regional scale, it is not possible to measure field-scale parameters. In this study, the uncertainty ranges of most vegetation parameters were taken from the table in Dawes and Zhang (1998). Only a few parameter ranges were modified after a brief literature review to better reflect C3 annual pasture in a semi-arid environment in southeast Australia. These modified parameters are indicated in Table 2.

3.3 Model setup and recharge assessment

WAVES requires discretisation of the unsaturated zone in order to solve the Richards equation. In this study, the model was set up to be 4 m in depth with the top of the model representing the land surface. At the depth of 4 m, both soil evaporation and plant transpiration should become negligible given the maximum rooting depth of 1.5 m (Table 2) and the average water table depth of 10-15 m. Hence deep drainage can be assumed to equal actual groundwater recharge. The bottom of the model was specified with a free drainage boundary condition. The model was discretised into 58 elements with the elemental size increasing from 0.001 m near the top to 0.05 m at a depth of 0.4 m. From 0.4 m to 4 m, a constant elemental size of 0.1 m was used. The top 0.3 m was assumed to be the topsoil, whereas the remaining soil layer comprised the subsoil.

The initial matric potential was assumed to be uniform at -100 m and the initial root carbon mass was assumed to be 0.002 kg/m^2 at all nodes. The initial leaf carbon was set at 0.05 kg/m^2 and the stem carbon was 0.5 km/m^2. Because we do not know the exact initial

conditions, it takes some time for the model to spin up to the equilibrium state. We assessed the time for leaf area index to reach its long-term trend in several selected model realisations. Our assessment suggests that the spin-up time is only several years in those selected model realisations. Given the stochastic nature of this study, it is impossible to examine the spin-up time for all model realisations. As the period for simulation was 127 years starting from 1889 (first year data is available), we chose the last 50 years to calculate the long-term average groundwater recharge and left the first 77 years for the model to spin up. Such a long time should allow any model realisation to reach its equilibrium state.

The input vegetation parameters were sampled from the parameter ranges listed in Table 2 using the Monte Carlo approach. The Latin Hypercube sampling technique was used to perform stratified sampling of all parameters which ensured the reasonable distribution of samples over a sampling space. In comparison to simple Monte Carlo sampling, this stratified sampling approach requires less realisations to describe a probability distribution. Given the large number of uncertain parameters, 40,000 realisations were generated to yield 40,000 recharge estimates (i.e., 10,000 realisations for each group of soil hydraulic parameters). In theory, the number of realisations should be dependent on the particular case to ensure ergodic statistics. In this study, we chose 40,000 realisations based on the computational power we could access and this number is more likely to capture many important parameter sets than a smaller number. The soil hydraulic parameters were chosen from the four groups derived from four different pedotransfer functions (Table 1).

After sampling, all parameters and variables were fed into the WAVES model to simulate daily drainage. The long-term mean groundwater recharge was estimated by taking the average of daily drainage over the past 50 years (i.e., 1966-2016).

3.4 Sensitivity analysis

A sensitivity analysis is useful for determining influential model parameters. Often, an exhaustive assessment requires a number of sensitivity analysis methods to distinguish different groups of parameters, i.e., parameters with negligible effects, linear effects, nonlinear and/or interaction effects. In this study, the purpose of the sensitivity analysis was to improve qualitative understanding of those parameters rather than an exhaustive assessment. Hence, we only carried out one sensitivity analysis.

The Morris method was chosen to perform the sensitivity analysis (Morris, 1991; Saltelli et al., 2008). This method normalises the parameter space to the multidimensional hypercube (i.e., each dimension represents one parameter). Each dimension is divided into the same number of intervals, which equals the number of scenarios. For each scenario, the Morris method randomly decides the trajectory in the parameter space. One measure μ^* (mean of the elementary effects of a parameter, i.e., the ratios of recharge change to parameter change) is calculated for every parameter.

In this study, we analysed the sensitivity of the vegetation parameters and soil hydraulic parameters. The ranges of the vegetation parameters are the same as those in Table 2. Unlike the vegetation parameters, the soil hydraulic parameters are not independent. These parameters appear in groups as shown in Table 2. As the sensitivity analysis requires parameter ranges, we chose the subsoil in Table 1 as an example and determined the ranges of the soil hydraulic parameters from the highest and lowest values. Hence, the ranges for K_s, θ_s, θ_r and λ_c are 0.00634 - 0.189 m/d, 0.327 - 0.428, 0.128 - 0.306 and 0.0428 - 0.296 m, respectively. The parameter C is treated constant, as it was estimated to be 10 from all the

pedotransfer functions. Moreover, our initial testing suggests recharge is also insensitive to C. Although we did not examine soil hydraulic parameters from different soil layers and soil groups, the sensitivity analysis is still indicative of the importance of these soil hydraulic parameters in the model.

3.5 Model calibration

We examined uncertainty in recharge using both uncalibrated and calibrated models (Figure 2). Calibrated models use ET and/or soil moisture for calibration, as these parameters have been most often used for model calibration in the literature (Chen et al., 2014; Cheng et al., 2014; Kendy et al., 2003). Soil moisture content can be easily measured by installing moisture sensors at depth of interest. Evapotranspiration can be inferred from meteorological data or from satellite imagery. Hence, in this study, we also attempt to evaluate whether soil moisture content and evapotranspiration time series can reduce recharge uncertainty.

In order to produce generalised results, the soil moisture and ET data were obtained from one realisation with parameters randomly sampled (Figure 2). In this study, we only extracted the last 10 years of the time series produced from the specific realisation, as our experience indicates that it is rare to have more than 10 years of field data. The synthetic time series was then treated as observations for model calibration. To account for observational uncertainty arising from human errors, equipment errors or analysis errors, we added 10% error to the synthetic time series shown as upper and lower bounds in Figure 3. This is towards the lower level of ET measurement errors reported in the literature (Glenn et al., 2011). Congruent information for soil moisture does not exist, although in our judgement 10% represents a reasonable estimate of uncertainty involved in field sampling and analysis for soil moisture (e.g., different sensor types, local-scale soil heterogeneity and operational errors). To allow

for consistent framework and quantitative comparison, we therefore applied the same percent error to soil moisture. We therefore consider a model fitting error to occur only when the simulated value differs from the original value by more than 10% (Figure 3).

Goodness of fit can be examined using statistical variables. These include (1) Root mean squared error (RMSE), a measure of the average differences between modelled results and observed results. Smaller RMSE indicates better prediction of the model. (2) Mean relative error (MRE), a measure of the bias of the modelled results compared to observed ones. MRE > 0 is a sign of model over-prediction and MRE < 0 signals model under-prediction. (3) Coefficient of determination (R^2), a measure of the agreement between observed and modelled results. High R^2 indicates strong goodness of fit, whereas low R^2 suggests weak model fitting to measured results. The formulae are

$$RMSE = \sqrt{\frac{1}{n}\sum_{i=1}^{n}(P_i - O_i)^2} \quad (1)$$

$$MRE = \frac{1}{n}\sum_{i=1}^{n}\left|\frac{P_i - O_i}{O_i}\right| \quad (2)$$

$$R^2 = \frac{\left[\sum_{i=1}^{n}(P_i - \overline{P})(O_i - \overline{O})\right]^2}{\sum_{i=1}^{n}(P_i - \overline{P})^2 \sum_{i=1}^{n}(O_i - \overline{O})^2} \quad (3)$$

where P_i and O_i are predicted and observed values, respectively, and $\overline{P}$ and $\overline{O}$ are average values of the predicted and observed time series, respectively. Note that Nash–Sutcliffe Model Efficiency (NSE) is another metric that measures model sensitivity to outliers. Because the similarity between NSE and RMSE, NSE was not included here.

Criteria must be used to determine acceptable models. In this study, we first computed the mean and standard deviation of synthetic time series. We then used half of the standard deviation as the cut-off for RMSE and 0.5 for R^2 in accordance with Moriasi et al. (2007). The criteria provided by Moriasi et al. (2007) were based on a thorough review of catchment modelling studies. In addition, we used half of the coefficient of variation (the ratio of the standard deviation to the mean) for MRE in order to link it to observations (i.e., baseline data in this study). A model is deemed as acceptable only if all the three fit statistics meet their criteria at the same time. Although there is general guidance in the literature, the choice of cut-off criteria is still subjective.

4. Results

4.1 A demonstrative example

Figure 4 shows the partitioning of the water input (i.e., rainfall) into several different water-budget components over a period of 10 years. The long-term average rainfall was 398 mm/y. Most rain was less than 40 mm/d and fell between June and August. Heavy rain as much as 60 mm/d or more occurred in some years. The average interception rate was 118 mm/y, about 30% of the rainfall, with the average leaf area index of 0.801. This interception rate is reasonable as the study area is semi-arid and most rainfall is below 20 mm/d. Clark (1940) showed that wheat (functionally same as annual pasture) can intercept more than 33% of rainfall when rainfall is less than 1.48 inches/d (i.e., 38 mm/d). Any water that was not intercepted by leaves would reach the ground and undergo further partitioning. Heavy rainfall tended to cause overland flow, especially when the rainfall exceeded about 20 mm/d. The average overland flow rate was 36 mm/y. Once the water entered the soil, it migrated through the soil pores to increase the soil moisture storage, where a large part of the water was transpired back to the atmosphere by the plant through the stomata, or drained through the

root zone to recharge the underlying groundwater. The mean ET rate was about 183 mm/y, accounting for 45% of the rainfall. Note that this ET value only comprised soil evaporation and plant transpiration. The total ET is 301 mm/y, as it also includes canopy evaporation (i.e., rainfall interception).

The deep drainage through the root zone is the source of groundwater recharge. The long-term average drainage (61 mm/y) accounted for 15% of the rainfall. The drainage also exhibits a strong annual variation in addition to seasonal variation. For example, between the 3rd and 4th years, the recharge was relatively low and steady at approximately 0.1 mm/d, whereas the recharge spiked to 1.7 mm/d in the 9th year. The highest annual recharge occurred in the 6th year (162 mm/y), whereas the lowest was in the 4th year (17 mm/y).

4.2 Sensitivity analysis

The Morris sensitivity analysis suggests that maximum carbon assimilation rate (A_{max}), saturated hydraulic conductivity (K_s) and saturated water content (θ_s) and residual water content (θ_r) play more important roles than other parameters because of the higher mean values of the elementary effects (Figure 5). A_{max} is important as it affects the actual carbon assimilation rate which impacts on stomatal conductance. The other three important parameters (K_s, θ_s and θ_r) determine the capability of soil to transmit or retain soil water. It is not surprising that these parameters are important.

The next set of important parameters include rainfall interception coefficient (K_r), light extinction coefficient (k), saturation light intensity (L_{sat}), leaf respiration rate (L_{rate}), leaf mortality rate (M_{rate}) and above-ground partitioning factor (β). K_r determines how much rainfall will be intercepted by leaves and hence impacts on the availability of water reaching

the ground. Similarly, k affects the distribution of solar radiation and longwave radiation at different layers, which are the energy sources for evapotranspiration. The other four parameters (L_{sat}, L_{rate}, M_{rate} and β) play important roles in plant growth.

4.3 Recharge uncertainty

As with the demonstrative example, we generated 10,000 realisations by randomly sampling all the vegetation parameters. All the 10,000 realisations share the same climate inputs and use the same set of soil hydraulic parameters as those in the demonstrative example. 30,000 realisations were run later for the other three sets of soil hydraulic parameters. 10,000 realisations produced 10,000 values of long-term mean groundwater recharge. Note that the recharge produced from these realisations is direct output from WAVES without model calibration. As shown in Figure 6 (Pedo1), the possible recharge range is between 7 and 144 mm/y with the mean recharge at 66 mm/y.

Figure 6 also shows the differences in the recharge distributions and statistics between the four pedotransfer functions. Pedo2 and Pedo3 resulted in quite similar recharge ranges (7-80 mm/y), whereas the last pedotransfer function produced a much wider range (10-240 mm/y). The t-Test suggests that the difference in mean recharge is statistically significant between any two groups. The much wider recharge range in the fourth pedotransfer function is attributed to the larger saturated hydraulic conductivity and the larger residual water content, using the Rosetta program (Schaap et al., 2001). Because of the fourth pedotransfer function, the overall recharge range increased from 7-144 mm/y to 7-236 mm/y. The upper bound of the recharge range has increased by 92 mm/y. The 236 mm/y for recharge was for an extreme parameter combination (e.g., high K_s, small difference between θ_s and θ_r, low A_{max}). Such a high recharge value is unlikely to be realistic for a semi-arid environment, and the probability

for it to occur is very low. The large range of recharge estimates in Figure 6 indicates that this method is unlikely to produce highly constrained recharge that can be confidently used by water resources managers. Note that we present several recharge statistics in Figure 6b and several following figures, but our analysis throughout this study is focused on the complete recharge range (i.e., the range between minimum and maximum values rather than 5-95 percentiles or 25-75 percentiles).

4.4 Model calibration

To test our hypothesis that additional datasets may help to reduce recharge uncertainty, we chose a single realisation (as a base case) to generate a moisture content time series at the 0.6m depth and ET time series. Both moisture content and ET time series are used to calibrate the WAVES models in order to produce constrained recharge estimates. Note that the choice of 0.6 m for the moisture content is subjective. Any other depths could also be used to perform this analysis. As the depth of 0.3 m is defined as the interface between topsoil and subsoil, this 0.6 m depth is located in the subsoil. The two time series for the last 10 years were extracted and modified by adding lower and upper error bounds (±10% of the actual values) as outlined in the Methods section. The synthetic curves in Figure 7 show the error bounds of the moisture content and the ET time series for the last 10 years. It should also be noted that the synthetic ET time series in the following analysis only includes soil evaporation and plant transpiration. Actual ET measurements should also include rainfall interception by canopies. Given a theoretical study, the use of ET time series without including rainfall interception is not expected to have a significant impact on the conclusions.

Figure 7 also shows the modelled moisture content and ET from three different model realisations using different parameter values. These three model realisations produce different

groundwater recharge but they all provide a reasonable fit to the data produced from the base case. As can be seen, the overall fitting for both moisture content and ET was quite reasonable. Take Model 1 for example, RMSE, MRE and R^2 for soil moisture are 0.0, 0.0 and 1.0, respectively, considering the error bounds (Figure 7a) and RMSE, MRE and R^2 for ET are 0.207 mm/d, 0.247 and 0.856, respectively. The quantitative measures indicate the fitting is better for moisture content than for ET, consistent with the qualitative inspection.

This process of data fitting was carried out 40,000 times. Each fit statistic can be used to determine the plausible range of the recharge by examining the relationship between the statistic and the recharge (Figure 8). For RMSE and MRE, the data points were separated into 3-4 clusters and spread in a similar fashion to the relevant recharge distribution in Figure 6. The spreading was likely caused by relatively stable moisture content (i.e., moisture content stabilises at the residual moisture content for more than half of the time as shown in Figure 7). This is because our synthetic dataset was generated by using one of the four groups of the soil hydraulic parameters. The other three groups of the soil hydraulic parameters seem to produce different soil moisture results regardless of vegetation parameters.

As the mean and the standard deviation of the synthetic data are 0.248 and 0.015, respectively, we used half of the standard deviation (0.007), half of the coefficient of variation (0.03) and 0.5 as the cut-off values for RMSE, MRE and R^2, respectively, as explained in the Methods section. A model is acceptable only if the three fit statistics meet their cut-off criteria at the same time. Hence, the final recharge range is 7 – 144 mm/y (θ, Figure 9) with 9,999 acceptable models (θ of Test Case 1, Table 3), nearly half of the range without data fitting. However, as shown on the right panel of Figure 8, the acceptable models are from the same cluster. These acceptable models used the same group of soil hydraulic parameters as the

base case that produced the synthetic time series, and only one of the 10,000 realisations that used these soil parameters was deemed to be unacceptable. If only realisations using the same soil parameters are used, then calibration to soil moisture does not provide any constraint on groundwater recharge. This is attributed to the narrow variation in soil moisture content relative to the measurement error (Figure 7).

The ET time series was used to constrain the recharge range in the same manner as the soil moisture time series. As the mean and the standard deviation of the synthetic data are 0.546 and 0.503 mm/d, respectively, we used half of the standard deviation (0.252), half of the coefficient of variation (0.46) and 0.5 as cut-off values for RMSE, MRE and R^2, respectively, as explained in the Methods section. The Monte Carlo simulations produced a range of values for fit statistics, and we examined the relationships between these and recharge (Figure 10). The plausible range of recharge resulting from the combination of the fit statistics is between 33 and 113 mm/y (ET, Figure 9) and the number of acceptable models is 2,107 (ET of Test Case 1, Table 3). The ET produced a narrower range of recharge than the soil moisture in this specific test case.

When both the soil moisture and ET were used together to calibrate the model, the recharge range was not significantly reduced from that produced from calibration to ET alone (θ + ET, Figure 9). However, the number of acceptable models reduced to 1,543 (θ + ET of Test Case 1, Table 3). Clearly, in this synthetic scenario, the recharge range was narrowed from 7-236 mm/y to 33-113 mm/y through data fitting. As shown in Figure 7, both the cases producing 33 and 113 mm/y recharge can fit the synthetic time series equally well.

In order to investigate whether the ability of data fitting to reduce recharge uncertainty is dependent on the base case chosen, the data fitting process was repeated twice using different base cases. The first base case produced a recharge range of 34-119 mm/y (Figure 11a), whereas the second base case yielded a recharge range of 26-145 mm/y (Figure 11b). As with test case 1, both the test cases here also show the decrease in the number of acceptable models as we used different datasets for model calibration (Test Cases 2 and 3, Table 3).

Although it is clear that model calibration will usually be able to reduce the uncertainty of recharge, the degree of uncertainty reduction is expected to be correlated with the potential error of a dataset used for calibration. To investigate this, we repeated the calibration to ET, but with varying the error associated with the data. Thus, if the error on the ET dataset is increased from 10% to 30%, the range in estimated recharge increases from 33-113 to 22-236 mm/y (Figure 12). The recharge range narrows steadily as the error decreases, and for a 5% error in ET, the recharge range becomes 37-111 mm/y.

5. Discussion

Water and energy balance models are useful to address climate change impacts on ecohydrology. For the purpose of estimating recharge, such models may have large uncertainty, as demonstrated in this study using the WAVES model. The challenge in using the WAVES model to estimate recharge lies in the reliable determination of parameters. There were 26 parameters and 4 soil hydraulic parameters required by the WAVES model. The uncertainties of these parameters resulted in the large uncertainty range of the long-term average groundwater recharge. Through several hypothetical cases, however, we demonstrated that the groundwater recharge uncertainty could be narrowed down by fitting commonly measured variables such as ET but not soil moisture content. Whether the

recharge rates estimated from the calibrated models are sufficiently accurate will depend on the uncertainty of the calibration data and the purpose of the investigation.

5.1 Soil hydraulic properties

Pedotransfer functions are often used to translate soil texture information to soil hydraulic parameters in unsaturated zone modelling (Hohenbrink and Lischeid, 2014; Wang et al., 2015). A large number of pedotransfer functions are available (Vereecken et al., 2010), with the Rosetta program being the most widely used (Schaap et al., 2001). However, most pedotransfer functions were developed to yield retention curve parameters only, and some of them require soil particle distribution that we do not possess. In the end, four pedotransfer functions were employed to infer both retention curve parameters and saturated hydraulic conductivity (Dane and Puckett, 1992, Saxton et al., 1986, Wösten et al., 1999 and Schaap et al., 2001). We discovered that different pedotransfer functions resulted in differences in soil hydraulic properties (Table 1). Different groups of soil hydraulic properties resulted in the different ranges of recharge estimates (Figure 6). The combination of these different groups of soil hydraulic properties led to the large uncertainty range of recharge. This conclusion is in accord with results from previous investigations that have concluded that different pedotransfer functions can result in up to an order of magnitude difference in recharge estimates (Faust et al., 2006).

The large uncertainty in recharge was more likely caused by the combination of large K_s and small difference between θ_s and θ_r for both the topsoil and subsoil (see Pedo4 in Table 1). This is because the small difference between θ_s and θ_r allows the soil to reach saturation with only a small amount of water and the large K_s permits fast transmission of water in the soil. For a semi-arid environment with limited precipitation, reaching saturation faster will allow

water to infiltrate through the root zone faster and hence will result in more deep drainage. This important information was not reflected by the sensitivity analysis as the two parameters were treated as independent parameters. This suggests that even if we cannot determine θ_s and θ_r precisely, efforts should be devoted to reduce the uncertainty of the difference between these two parameters. In comparison, the sensitivity analysis showed K_s is indeed important. This parameter can be determined through several techniques such as pumping tests and slug tests. However, it often ranges over several orders of magnitude.

To reduce the uncertainty of soil hydraulic properties, it is best to develop pedotransfer functions for the study region. Wösten et al. (2001) concluded that pedotransfer functions are better used for making predictions for the area where the soils were sampled to derive the functions. At the scale of this study, it may seem feasible to develop our own pedotransfer functions. However, at regional scales (e.g., Crosbie et al., 2010) or when a project is time- and budget-limited, the development of pedotransfer functions does not seem practical. Hence, many studies tend to seek established pedotransfer functions to save time and budget (Cornelis et al., 2001; Sobieraj et al, 2001). To select the most appropriate pedotransfer functions, field observations such as soil moisture may also be helpful, because different pedotransfer functions may correlate to different soil moisture variations. In our study, we attempted to directly reduce recharge uncertainty by fitting modelled to synthetic moisture content time series. The modelling showed only those models that use the same group of soil hydraulic parameters as that generated the synthetic time series were acceptable. While in reality observed moisture content may not inform us the exact pedotransfer function, it should be able to indicate which one is most probable.

5.2 Vegetation parameters

In this study, we adopted the vegetation parameter ranges from the WAVES manual with slight adjustment. Many parameters for specific plants can be measured in the field or in the lab. As we attempted to cover the category of C3 annual pasture instead of a specific plant at the regional scale, our approach was deemed appropriate and the parameter ranges were reasonable. This is a common practice in many water and energy balance models classifying the terrestrial biosphere into limited number of plant functional types (Grace and Williams, 2004). However, the uncertainty range of groundwater recharge is likely to be large due to the uncertainty in different parameters.

To reduce the uncertainty of recharge, the first approach is to reduce the uncertainties of several important vegetation parameters. A sensitivity analysis can be undertaken to identify these parameters (e.g., A_{max}, K_r and k in Figure 5) and dedicate relevant efforts to improve measurements. Similar to soil hydraulic properties, this is only feasible at point scales (i.e., for individual plant species). At large scales, plant functional types (e.g., annual, perennial, evergreen and deciduous) are usually used. Each plant functional type includes many different plant species. Estimating parameters for a plant functional type would require a large number of measurements for all the different species. More importantly, there is no guarantee of lowering parameter uncertainty given the large number of plant species. Hence, the scope of reducing parameter uncertainty directly is very limited. The second approach is to directly reduce uncertainty of recharge by comparing to available observations. As shown in Figure 9 and Figure 11, ET narrowed the recharge down, whereas in our example soil moisture did not. ET is helpful because water and energy balance models essentially compute groundwater recharge as the residual of a water balance, where ET is further constrained by solving a simultaneous energy balance. With the availability of climate data and large-scale

satellite measurements of energy balance proxies, reducing recharge uncertainty with independent ET estimates is a reasonable approach. Soil moisture was not helpful in our study because the assumed 10% error of moisture content is large relative to the temporal variation. However, soil moisture may be of more use in other soil types, where temporal variations in water content may be more pronounced.

5.3 Comparison to other water balance models

Most soil water balance models treat potential ET as an input along with rainfall. de Vries and Simmers (2002) pointed out that recharge is usually smaller than the uncertainty range of ET and so the estimated recharge is very uncertain. In comparison, water and energy balance models such as WAVES used in this study directly computes ET in accordance with atmospheric and canopy conditions. The ET measurements are used to constrain water and energy balance models (Figure 10). This direct calculation of ET is beneficial to situations where ET measurements are limited. Of course, our analysis also indicates that the uncertainty of datasets used for model calibration impacts on the uncertainty of recharge. Figure 12 shows that the reduction of ET uncertainty can greatly reduce the uncertainty of recharge.

A large number of water and energy balance models have been developed. Depending on the purposes, the complexity of these water and energy balance models and relevant equations used may differ. Nevertheless, all water and energy balance models simulate point-scale processes, i.e., transfer of heat and water occurs in the vertical direction. Hence, control points are usually needed to estimate recharge at point scales which are up-scaled to the relevant region using simple upscaling methods (Healy et al., 2012; Crosbie et al., 2013). Although the use of water and energy balance models to estimate groundwater recharge is

conceptually similar to simple soil water balance models, these water and energy balance models require a large number of parameters as discussed above and as a consequence increase the number of uncertainty sources. Whether this complexity is necessary for estimating groundwater recharge requires further assessment.

Moreover, many water and energy balance models treat the unsaturated zone as several buckets at different depths rather than solving Richards' equation to obtain vertical distribution of moisture content as WAVES. This treatment makes it hard to use soil moisture measured at specific depths to constrain models. Hence, the choice of a model needs to be based on the objective of a project and availability of datasets. As pointed out by Alley (1984), Gee and Hillel (1988) and Sorensen et al. (2014), models that treat soil layers as several reservoirs are likely to produce differing recharge estimates, because of different approaches used for water budget partitioning. Sorensen et al. (2014) demonstrated that soil moisture data alone are unable to constrain groundwater recharge in four commonly used water balance models, consistent with our study.

6. Conclusions

Water and energy balance models have become increasingly popular for estimating groundwater recharge. This is because these models attempt to simulate several balances (water, energy and carbon) at the same time and the additional balances are thought to constrain the water balance. However, the inclusion of the additional balances also introduce additional parameters that carry different degrees of uncertainty and likely complicate the estimation of recharge. This study is aimed to examine the uncertainty of groundwater recharge estimated from a typical water and energy balance model. The results showed that uncalibrated models have large uncertainty in recharge. However, for model calibration, soil

moisture time series may not offer much help for constraining models and reducing recharge uncertainty, whereas ET time series are able to reduce recharge uncertainty by more than 50%. The ability of a data time series to constrain models is dependent on its uncertainty relative to the magnitude of its temporal variation.

Acknowledgements

The authors are grateful to the Murray-Darling Basin Authority for the financial support for this project. This study also benefitted from discussions with Dr John Hutson from Flinders University, Dr Lu Zhang from CSIRO Canberra, and Professor Derek Eamus from the University of Technology Sydney.

Table and figure captions

Table 1. Four groups of soil hydraulic parameters using different sets of pedotransfer functions. Each group includes a topsoil (0 – 0.3 m) and a subsoil (below 0.3 m). Each topsoil or subsoil has five parameters: saturated hydraulic conductivity K_s (m/d), saturated water content θ_s (cm^3/cm^3), residual water content θ_r (cm^3/cm^3), macroscopic capillary length scale λ_c (m) and a soil structure parameter C (-). λ_c is inversely proportional to a flow-weighted mean pore size, whereas C is related to the slope of the moisture characteristic at satiation.

Table 2. Parameters used by WAVES for C3 annual pasture. The parameters that have been changed from the original table in Dawes and Zhang (1998) are marked with "*". Note that only those parameters with different upper and lower bounds were evaluated in the sensitivity analysis.

Table 3. Numbers of acceptable models and recharge ranges for three test cases that use soil moisture (θ), ET or the combination of both for model calibration. There were a total of 40,000 realisations. N columns show acceptable models, 90% columns show recharge ranges between 5 and 95 percentiles, and 100% columns show full recharge ranges. Test Case 1 corresponds to Figure 9 and Test Cases 2 and 3 correspond to Figure 11.

Figure 1. Geographic location of the study area in southeast Australia and distribution of two soil groups within the study area. The total area of the catchment is 7949 km^2.

Figure 2. Flow chart of groundwater recharge estimation using the WAVES model for one scenario. The flow chart without the dashed box is the regular process without model calibration, whereas the component in the box indicates the process of the model calibration adopted in this study. For the Monte Carlo analysis (40,000 scenarios), the uncertain parameters outside the dashed box were randomly sampled every time, whereas those within the box (marked with *) were sampled only once and fixed throughout the entire Monte Carlo process.

Figure 3. A schematic of observational errors and fitting errors. The observation errors are indicated in the shaded area. The fitting errors depend on the location of simulated values. If a simulated value falls above the upper bound, the error will be the difference between the simulated value and the upper bound. Likewise, if the simulated value is below the lower bound, the error will be the difference between the simulated value and the lower bound. If the simulated value lies between the upper and lower bounds, there will be no error.

Figure 4. Flux variations in precipitation (P), rainfall interception (I), soil evaporation and plant transpiration (ET), overland flow (O) and drainage (D) in a single realisation. The 10 year period is between 2006 and 2016. In this example, the soil hydraulic parameters from Function Type 1 were used (Table 1).

Figure 5. Analysis of the WAVES model sensitivity to the parameters using the Morris method. μ^* shows the mean of the elementary effects of each parameter.

Figure 6. Histograms and boxplots of recharge estimates resulting from the uncertainty of vegetation parameters for different pedotransfer functions. In Figure b, the red bar within a box shows median recharge, the lower and upper sides of the box show 25 and 75 percentiles, the lower and upper bars outside the box show 5 and 95 percentiles, and the thick lines (clusters of dots) indicate recharge estimates lower than 5 and greater than 95 percentiles.

Figure 7. Comparison between the synthetic and modelled time series for 10 years (2006-2016). The moisture content time series was at 0.6 m depth. The synthetic data time series were created from a forward model run with randomly sampled parameters. The shaded areas adjacent to the synthetic data time series represent 10% errors. The fit statistics are shown in Figure 8 and Figure 10 below. The long-term average recharge for the synthetic base case is 76 mm/y. Models 1-3 are examples of models with different recharge rates that fit the data equally satisfactorily. The recharge for Model 1, 2 and 3 is the median value (68 mm/y), the lower bound (33 mm/y) and the upper bound (113 mm/y) of the acceptable range (θ + ET, Figure 9), respectively. Note that the inset plots in both (a) and (b) show the close-up of the moisture content and ET between 1.9 and 2.1 years, respectively. The supplementary material provides more detailed and clearer comparison of soil moisture content and ET.

Figure 8. Different fit statistics for soil moisture content, plotted against simulated values of groundwater recharge. The two plots at each row are the same, except that the one on the right shows all the acceptable models defined by the cut-off value of the fit statistic (i.e., the cut-off values are 0.007, 0.028 and 0.5 for RMSE, MRE and R^2, respectively). The three dots shown in red, blue, and green are the fit statistics of the three model realisations in the same colours shown in Figure 7.

Figure 9. Reduction in the recharge uncertainty with data fitting. For the x-axis, No Fitting, θ, ET and θ + ET show recharge statistics without any model calibration, after model calibration to soil moisture content, after model calibration to evapotranspiration, and after model calibration to both soil moisture content and evapotranspiration, respectively. For each boxplot, the red bar within the box show median recharge, the lower and upper sides of the box show 25 and 75 percentiles, the lower and upper bars outside the box show 5 and 95 percentiles, and the thick lines (clusters of dots) indicate recharge estimates beyond 5 and 95 percentiles. The full ranges and the ranges at 5-95 percentiles are also shown in Table 3.

Figure 10. Different fit statistics for ET, plotted against simulated values of groundwater recharge. The two plots at each row are the same, except that the one on the right shows all the acceptable models defined by the cut-off value of the fit statistic (i.e., the cut-off values are 0.25 mm/d, 0.46 and 0.5 for RMSE, MRE and R^2, respectively). The three dots shown in red, blue, and green are fit statistics of the three model realisations in the same colours shown in Figure 7.

Figure 11. Reduction in the recharge uncertainty with data fitting for two additional test cases. For each x-axis, No Fitting, θ, ET and θ + ET show recharge statistics without any model calibration, after model calibration to soil moisture content, after model calibration to evapotranspiration, and after model calibration to both soil moisture content and evapotranspiration, respectively. For each boxplot, the bar within the box show median recharge, the lower and upper edges of the box show 25 and 75 percentiles, the lower and upper bars outside the box show 5 and 95 percentiles, and the thick lines (clusters of dots) indicate recharge estimates beyond 5 and 95 percentiles. The full ranges and the ranges at 5-95 percentiles are also shown in Table 3.

Figure 12. Reduction in the recharge uncertainty with the decrease in the ET error.

References

Akkermans, T. et al., 2012. Validation and comparison of two soil-vegetation-atmosphere transfer models for tropical Africa. Journal of Geophysical Research: Biogeosciences, 117, G02013.

Alley, W.M., 1984. On the Treatment of Evapotranspiration, Soil Moisture Accounting, and Aquifer Recharge in Monthly Water Balance Models. Water Resources Research, 20(8): 1137-1149.

Allison, G.B., Gee, G.W., Tyler, S.W., 1994. Vadose-Zone Techniques for Estimating Groundwater Recharge in Arid and Semiarid Regions. Soil Science Society of America Journal, 58(1): 6-14.

Bredehoeft, J., 1997. Safe Yield and the Water Budget Myth. Ground Water, 1997, 35 (6), 929.

Bredehoeft, J., 2002. The Water Budget Myth Revisited: Why Hydrogeologists Model. Ground Water, 2002, 40 (4), 340-345.

Broadbridge, P., White, I., 1998. Constant rate rainfall infiltration: a versatile non-linear model: I. analytical solution. Water Resources Research, 24,145–154.

Chen, C. et al., 2014. Modelling vegetation water-use and groundwater recharge as affected by climate variability in an arid-zone Acacia savanna woodland. Journal of Hydrology, 519, Part A: 1084-1096.

Cheng, L. et al., 2014. Impacts of elevated CO_2, climate change and their interactions on water budgets in four different catchments in Australia. Journal of Hydrology, 519, Part B: 1350-1361.

Chung, I., Sophocleous, M.A., Mitiku, D.B., Kim, N.W., 2016. Estimating groundwater recharge in the humid and semi-arid African regions: review. Geosciences Journal, 20(5), 731-744.

Clark, O.R., 1940. Interception of rainfall by prairie grasses, weeds and certain crop plants. Ecological Monographs, 10(2), 243-277.

Crosbie, R.S., McCallum, J.L., Walker, G.R., Chiew, F.H.S., 2010. Modelling climate-change impacts on groundwater recharge in the Murray-Darling Basin, Australia. Hydrogeology Journal, 18(7): 1639-1656.

Crosbie, R.S., McCallum, J.L., Walker, G.R., Chiew, F.H.S., 2012. Episodic recharge and climate change in the Murray-Darling Basin, Australia. Hydrogeology Journal, 20(2): 245-261.

Crosbie, R.S. et al., 2013. Potential climate change effects on groundwater recharge in the High Plains Aquifer, USA. Water Resources Research, 49(7): 3936-3951.

Cornelis, W.M., Ronsyn, J., Van Meirvenne, M., Hartmann, R., 2001. Evaluation of Pedotransfer Functions for Predicting the Soil Moisture Retention Curve. Soil Science Society of America Journal, 65(3): 638-648.

Dane, J.H., Puckett, W.E., 1992. Field soil hydraulic properties based on physical and mineralogical information. In: van Genuchten, M.Th., Leij, F.J., Lund, L. (Eds.), Proceedings of International Workshop on Indirect Methods for Estimating the Hydraulic Properties of Unsaturated Soils. University of California, Riverside, CA, pp.389-403.

Devlin, J., Sophocleous, M., 2005. The persistence of the water budget myth and its relationship to sustainability. Hydrogeology Journal, 13(4), 549-554.

de Vries, J.J., Simmers, I., 2002. Groundwater recharge: an overview of processes and challenges. Hydrogeology Journal, 10(1): 5-17.

Dash, C.J., Sarangi, A., Adhikary, P.P. et al, 2016. Soil water budgeting approach to quantify potential groundwater recharge from croplands and groundwater use in a semi-arid region. Environ Earth Sci, 75: 853.

Dripps, W.R., Bradbury, K.R., 2007. A simple daily soil–water balance model for estimating the spatial and temporal distribution of groundwater recharge in temperate humid areas. Hydrogeology Journal, 15(3): 433-444.

Faust, A.E., Ferré, T.P.A., Schaap, M.G., Hinnell, A.C., 2006. Can Basin-Scale Recharge Be Estimated Reasonably with Water-Balance Models? Vadose Zone Journal, 5(3): 850-855.

Finch, J.W., 1998. Estimating direct groundwater recharge using a simple water balance model – sensitivity to land surface parameters. Journal of Hydrology, 211(1–4): 112-125.

Glenn, E.P. et al., 2011. Actual evapotranspiration estimation by ground and remote sensing methods: the Australian experience. Hydrological Processes, 25(26), 4103-4116.

Gee, G.W., Hillel, D., 1988. Groundwater recharge in arid regions: review and critique of estimation methods. Hydrol Processes, 2, 255-266.

Giambelluca, T., Loague, K., Green, R., Nullet, M., 1996. Uncertainty in recharge estimation: impact on groundwater vulnerability assessments for the Pearl Harbor Basin, O'ahu, Hawai'i, U.S.A. Journal of Contaminant Hydrology, 23(1), 85-112.

Grace, J., Williams, M., 2004. Understanding and parameterizing the soil-water-atmopshere transfer through vegetation. In Unsaturated-zone Modeling Progress, Challenges and Applications.

Grayso, R., Argent, R., Nathan, R., McMahon, T., Mein, R., 1998. Hydrological Recipes: Estimation techniques in Australian Hydrology, CRC Catchment Hydrology, Monash University, Melbourne.

Gorelick, S., Zheng, C., 2015. Global change and the groundwater management challenge. Water Resources Research, 2015, 51(5), 3031-3051.

Healy, R.W., 2012. Estimating groundwater recharge. Cambridge University Press.

Healy, R.W., Cook, P.G., 2002. Using groundwater levels to estimate recharge. Hydrogeology Journal, 10(1): 91-109.

Hohenbrink, T.L., Lischeid, G., 2014. Texture-depending performance of an in situ method assessing deep seepage. Journal of Hydrology, 511: 61-71.

Isbell, R., 1996. The Australian soil classification. CSIRO Publishing.

Jeffrey, S.J., Carter, J.O., Moodie, K.B., Beswick, A.R., 2001. Using spatial interpolation to construct a comprehensive archive of Australian climate data. Environmental Modelling & Software, 16(4): 309-330.

Jie, Z., van Heyden, J., Bendel, D., Barthel, R., 2011. Combination of soil-water balance models and water-table fluctuation methods for evaluation and improvement of groundwater recharge calculations. Hydrogeology Journal, 19(8): 1487-1502.

Kendy, E. et al., 2003. A soil-water-balance approach to quantify groundwater recharge from irrigated cropland in the North China Plain. Hydrological Processes, 17(10): 2011-2031.

Kennett-Smith, A., Cook, P.G., Walker, G.R., 1994. Factors affecting groundwater recharge following clearing in the south western Murray Basin. Journal of Hydrology, 154(1): 85-105.

Kurtzman, D., Scanlon, B.R., 2011. Groundwater Recharge through Vertisols: Irrigated Cropland vs. Natural Land, Israel. Vadose Zone Journal, 10(2): 662-674.

Lanini, S., Caballero, Y., 2016. Groundwater recharge and associated uncertainty estimation combining multi-method and multi-scale approaches. 8th International Congress on Environmental Modelling and Software, Jul 2016, Toulouse, France. <hal-01326398>

McCallum, J.L., Crosbie, R.S., Walker, G.R., Dawes, W.R. 2010. Impacts of climate change on groundwater in Australia: a sensitivity analysis of recharge, 18: 1625–1638.

Minasny, B., McBratney, A.B., Bristow, K.L., 1999. Comparison of different approaches to the development of pedotransfer functions for water-retention curves. Geoderma, 93(3–4): 225-253.

Moriasi, D.N., Arnold, J.G., Van Liew, M.W., Bingner, R.L., Harmel, R.D., Veith, T.L., 2007. Model evaluation guidelines for systematic quantification of accuracy in watershed simulations. American Society of Agricultural and Biological Engineers, 50(3), 885-900.

Morris, M. D., 1991. Factorial sampling plans for preliminary computational experiments. Technometrics, 33, 161–174.

Overgaard, J., Rosbjerg, D., Butts, M.B., 2006. Land-surface modelling in hydrological perspective – a review. Biogeosciences, 3(2): 229-241.

Petropoulos, G., Carlson, T., Wooster, M., 2009. An Overview of the Use of the SimSphere Soil Vegetation Atmosphere Transfer (SVAT) Model for the Study of Land-Atmosphere Interactions. Sensors, 9(6): 4286.

Ridley, A.M., Simpson, R.J., 1994. Seasonal development of roots under perennial and annual grass pastures. Australian Journal of Agricultural Research, 45, 1077-1087.

Rushton, K.R., Eilers, V.H.M., and Carter, R.C., 2006, Improved soil moisture balance methodology for recharge estimation. Journal of Hydrology, 318, 379–399.

Rushton, K., Ward, C., 1979. The estimation of groundwater recharge. Journal of Hydrology, 41(3), 345-361.

Ruiz, L. et al., 2010. Water balance modelling in a tropical watershed under deciduous forest (Mule Hole, India): Regolith matric storage buffers the groundwater recharge process. Journal of Hydrology, 380(3–4): 460-472.

Saltelli, A. et al., 2008. Global Sensitivity Analysis: the Primer. John Wiley & Sons, Ltd. Pp312.

Saxton, K.E. , Rawls, W.J. , Romberger, J.S. , Papendick, R.I., 1986. Estimating generalized soil-water characteristics from texture. Soil Science Society of America Journal, 50(4):1031-1036.

Scanlon, B.R., Healy, R.W., Cook, P.G., 2002. Choosing appropriate techniques for quantifying groundwater recharge. Hydrogeology Journal, 10(1), 18-39.

Scanlon, B.R., Keese, K.E., Flint, A.L., Flint, L.E., Gaye, C.B., Edmunds, W.M., Simmers, I., 2006. Global synthesis of groundwater recharge in semiarid and arid regions. Hydrol. Process. 20, 3335-3370. DOI: 10.1002/hyp.6335.

Schaap, M.G., Leij, F.J., van Genuchten, M.T., 2001. ROSETTA: a computer program for estimating soil hydraulic parameters with hierarchical pedotransfer functions. J. Hydrol. 251, 163–176.

Sellers, P.J., Mintz, Y., Sud, Y.C., Dalcher, A., 1986. A Simple Biosphere Model (SIB) for Use within General Circulation Models. Journal of the Atmospheric Sciences, 43(6): 505-531.

Sobieraj, J.A., Elsenbeer, H., Vertessy, R.A., 2001. Pedotransfer functions for estimating saturated hydraulic conductivity: implications for modeling storm flow generation. Journal of Hydrology, 251(3–4): 202-220.

Sorensen, J., Finch, J., Ireson, A., Jackson, C., 2014. Comparison of varied complexity models simulating recharge at the field scale. Hydrological Processes, 28(4), 2091-2102.

Taylor, R.G. and Howard, K.W.F., 1996, Groundwater recharge in the Victoria Nile basin of east Africa: support for the soil moisture balance approach using stable isotope tracers and flow modelling. Journal of Hydrology, 180, 31–53.

Turkeltaub, T., Kurtzman, D., Bel, G., Dahan, O., 2015. Examination of groundwater recharge with a calibrated/validated flow model of the deep vadose zone. Journal of Hydrology, 522: 618-627.

Vereecken, H. et al., 2010. Using Pedotransfer Functions to Estimate the van Genuchten–Mualem Soil Hydraulic Properties: A Review. Vadose Zone Journal, 9(4): 795-820.

Wang, T., Franz, T.E., Zlotnik, V.A., You, J., Shulski, M.D., 2015. Investigating soil controls on soil moisture spatial variability: Numerical simulations and field observations. Journal of Hydrology, 524: 576-586.

Westenbroek, S.M., Kelson, V.A., Dripps, W.R., Hunt, R.J., and Bradbury,K.R., 2010, SWB—A modified Thornthwaite-Mather Soil-Water-Balance code for estimating groundwater recharge: U.S. Geological Survey Techniques and Methods 6–A31, 60 p.

Williams, M. et al., 1996. Modelling the soil-plant-atmosphere continuum in a Quercus–Acer stand at Harvard Forest: the regulation of stomatal conductance by light, nitrogen and soil/plant hydraulic properties. Plant, Cell & Environment, 19(8): 911-927.

Wohling, D.L., Leaney, F.W., Crosbie, R.S., 2012. Deep drainage estimates using multiple linear regression with percent clay content and rainfall. Hydrol. Earth Syst. Sci., 16(2): 563-572.

Wösten, J.H.M., Lilly, A., Nemes, A., Le Bas, C., 1999. Development and use of a database of hydraulic properties of European soils. Geoderma, 90(3-4), 169–185.

Wösten, J.H.M., Pachepsky, Y.A., Rawls, W.J., 2001. Pedotransfer functions: bridging the gap between available basic soil data and missing soil hydraulic characteristics. Journal of Hydrology, 251(3–4): 123-150.

Xu, C.-Y., 1997. Application of Water Balance Models to Different Climatic Regions in China for Water Resources Assessment. Water Resources Management, 11(1): 51-67.

Xu, C.-Y., Singh, V.P., 1998. A Review on Monthly Water Balance Models for Water Resources Investigations. Water Resources Management, 12(1): 20-50.

Zhang, L., Dawes W.R. (Eds.), 1998. WAVES–An Integrated Energy and Water Balance Model. Technical Report No. 31/98, CSIRO Land and Water, Canberra, Australia.

Zhang, L. et al., 1999. Estimating episodic recharge under different crop/pasture rotations in the Mallee region. Part 1. Experiments and model calibration. Agricultural Water Management, 42(2): 219-235.

Zhang, L., Walker, G.R., Dawes, W.R., 2002. Water balance modelling: concepts and applications. In: McVicar, T.R., Li Rui, Walker, J., Fitzpatrick, R.W. and Liu Changming (eds), Regional Water and Soil Assessment for Managing Sustainable Agriculture in China and Australia, ACIAR Monograph No. 84, 31–47.

Zhou, Y., 2009. A critical review of groundwater budget myth, safe yield and sustainability. Journal of Hydrology, 370(1), 207-213.

Zhang, H., Hiscock, K., 2010. Modelling the impact of forest cover on groundwater resources: A case study of the Sherwood Sandstone aquifer in the East Midlands, UK. Journal of Hydrology, 392(3), 136-149.

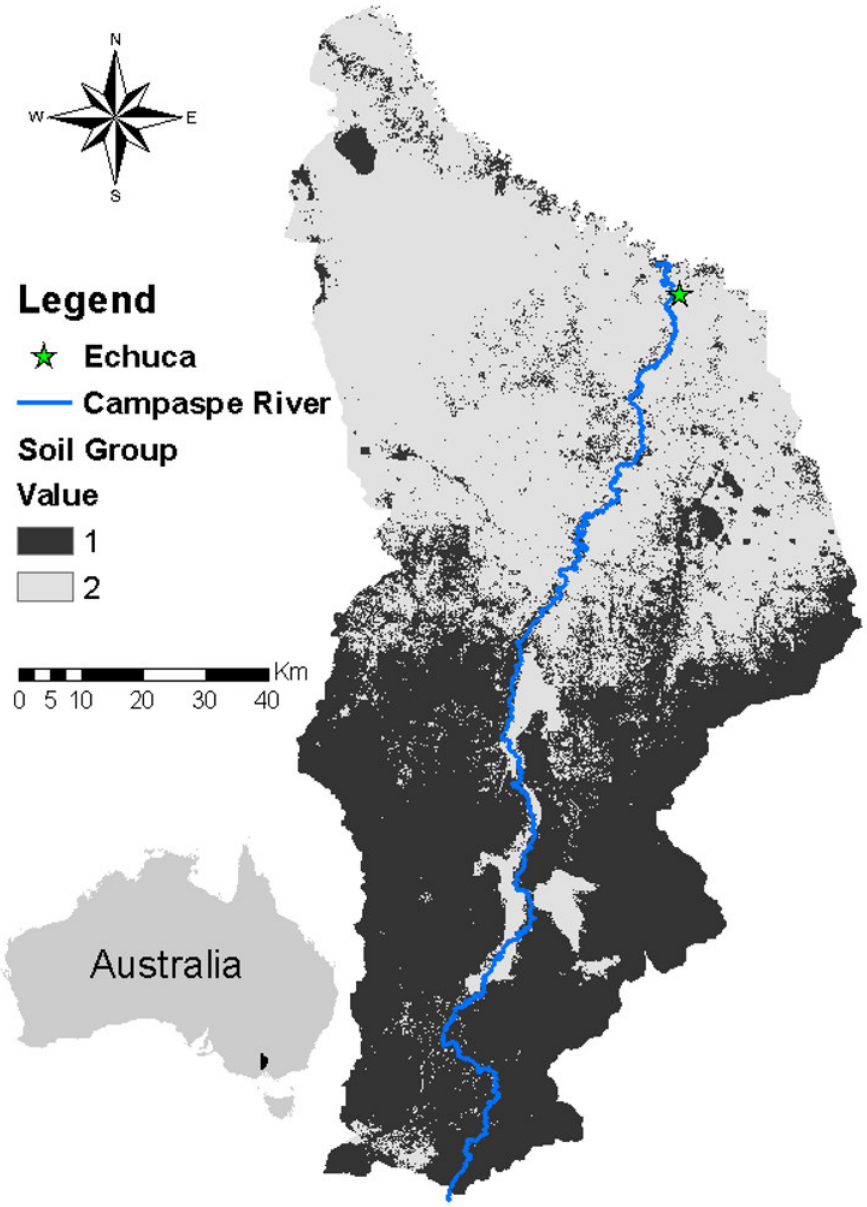

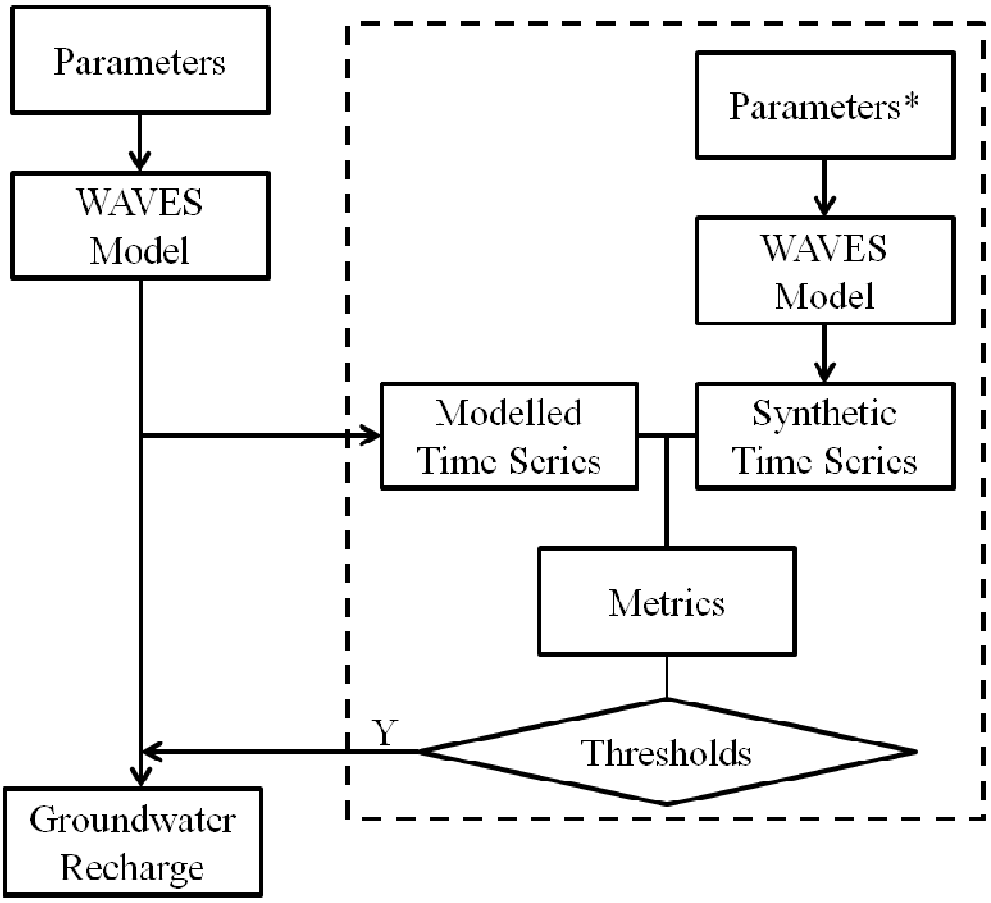

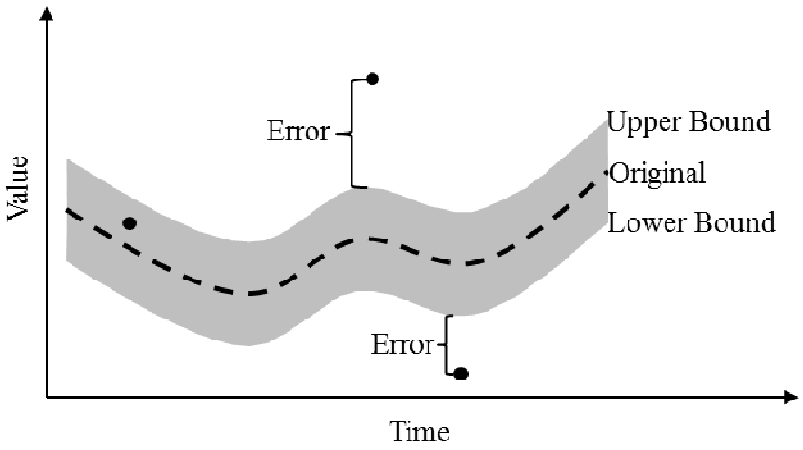

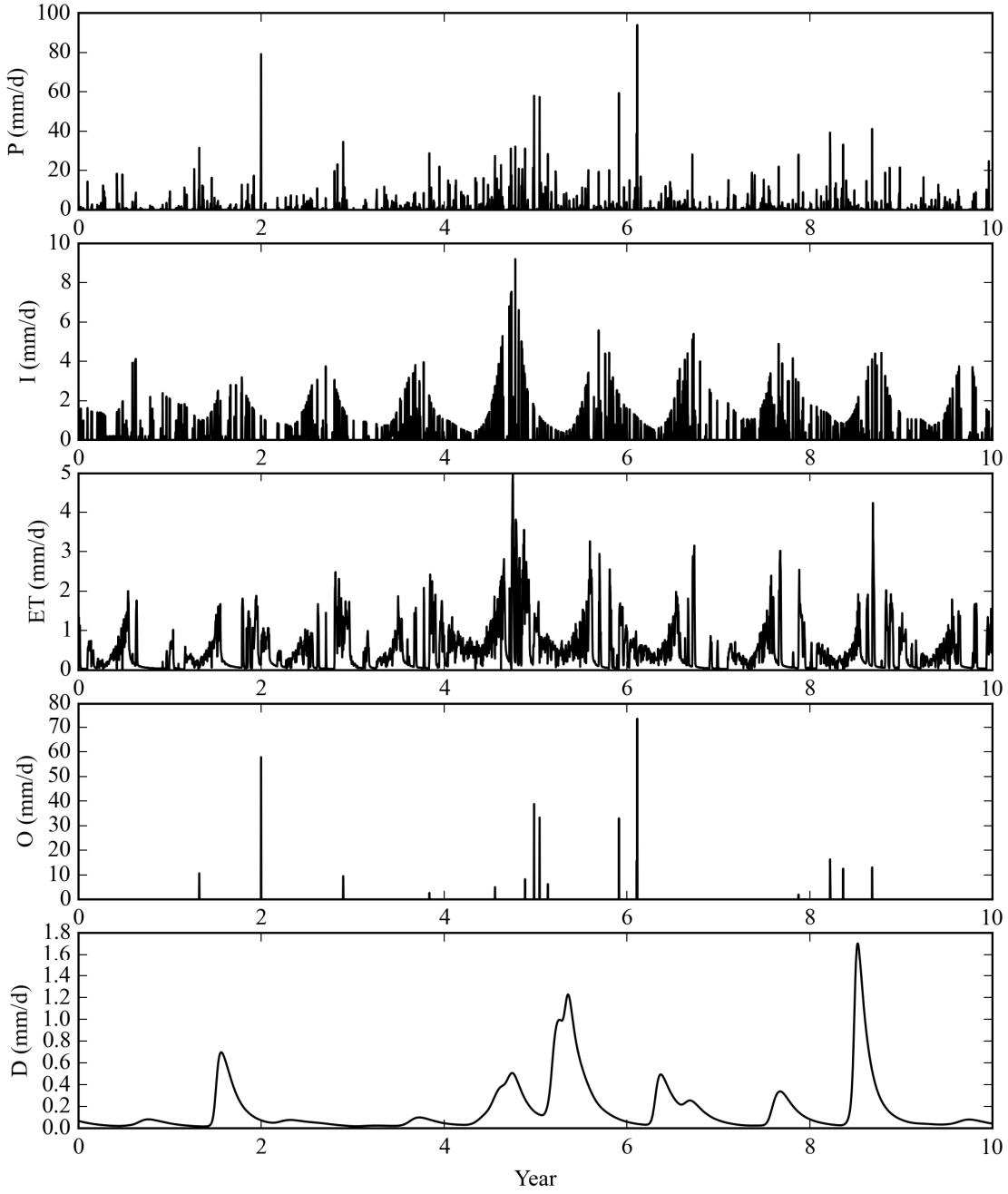
P (mm/d)
I (mm/d)
ET (mm/d)
O (mm/d)
D (mm/d)
Year

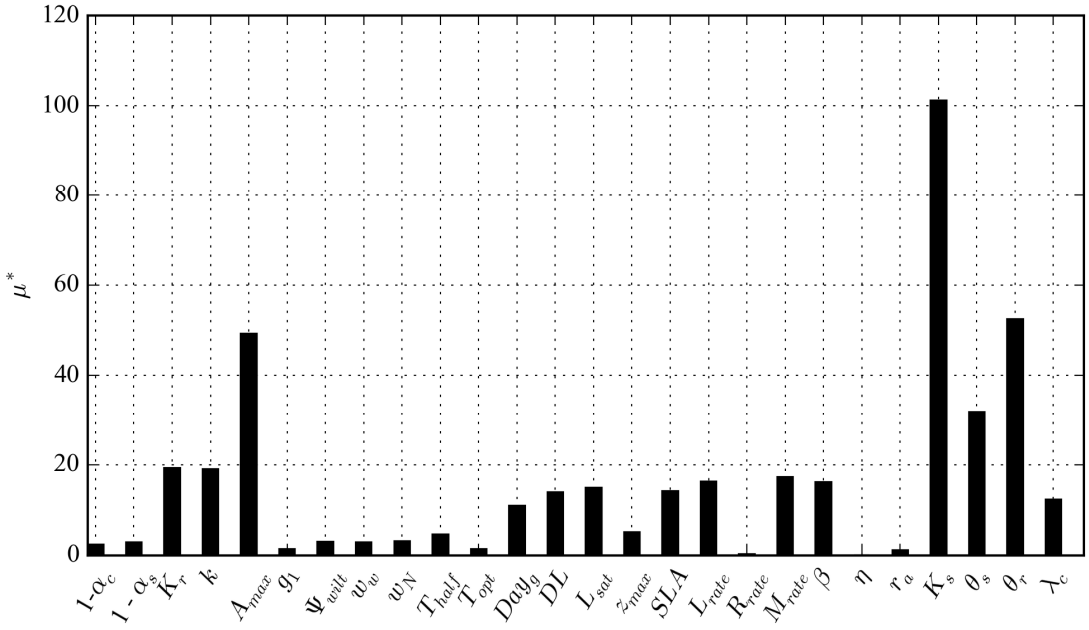

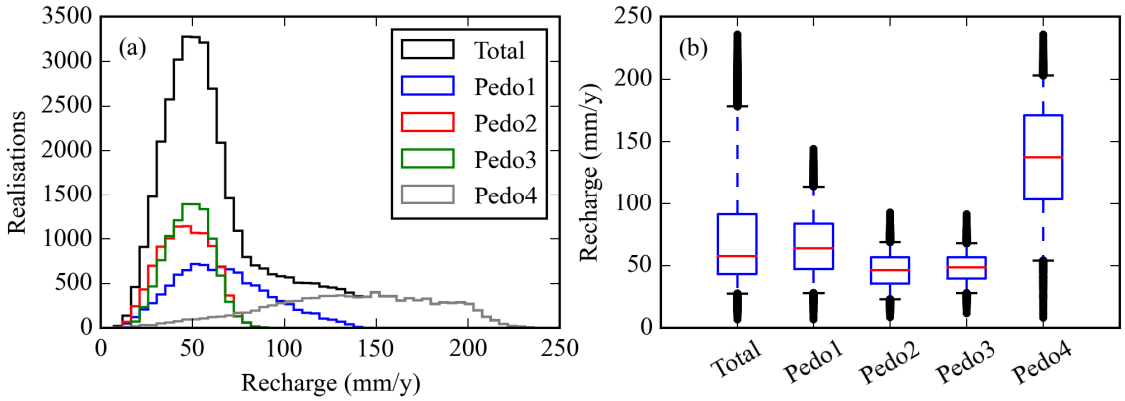

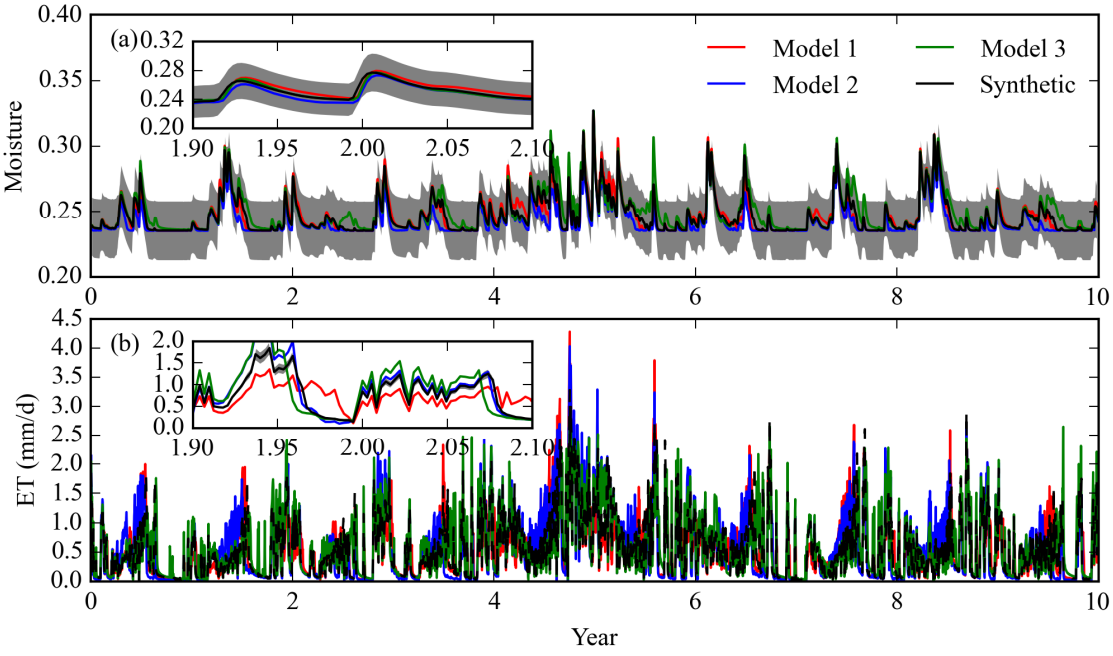

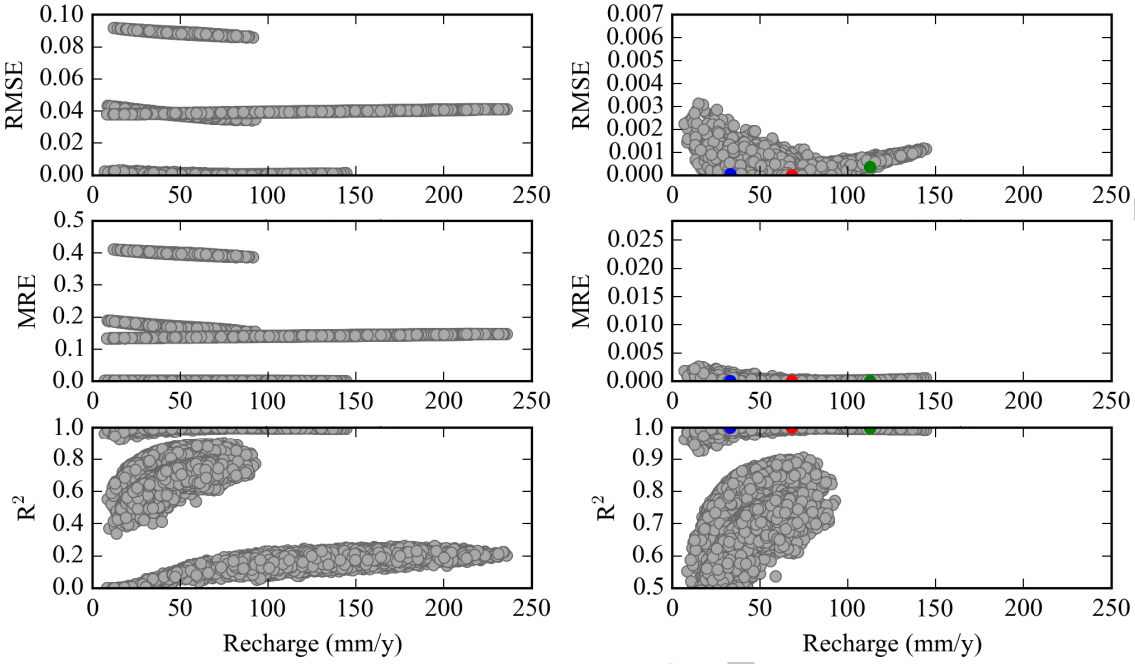

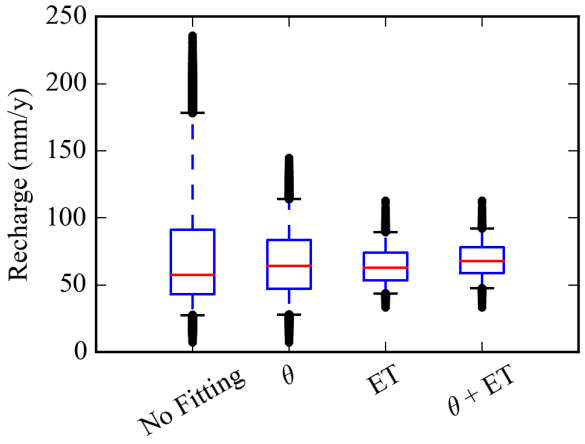

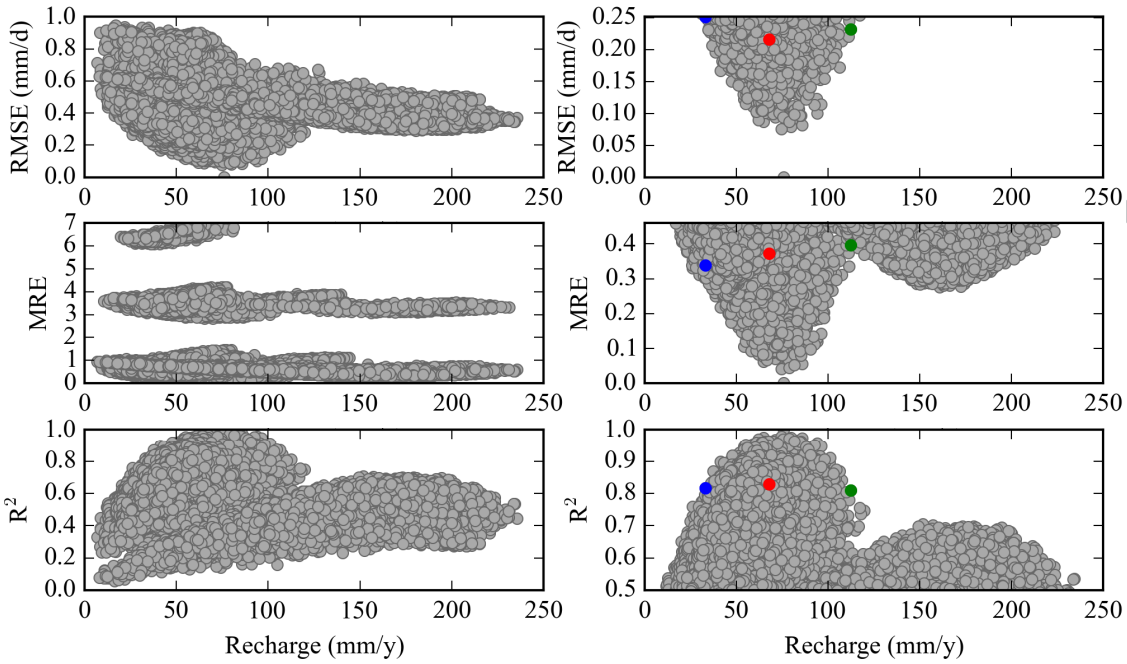

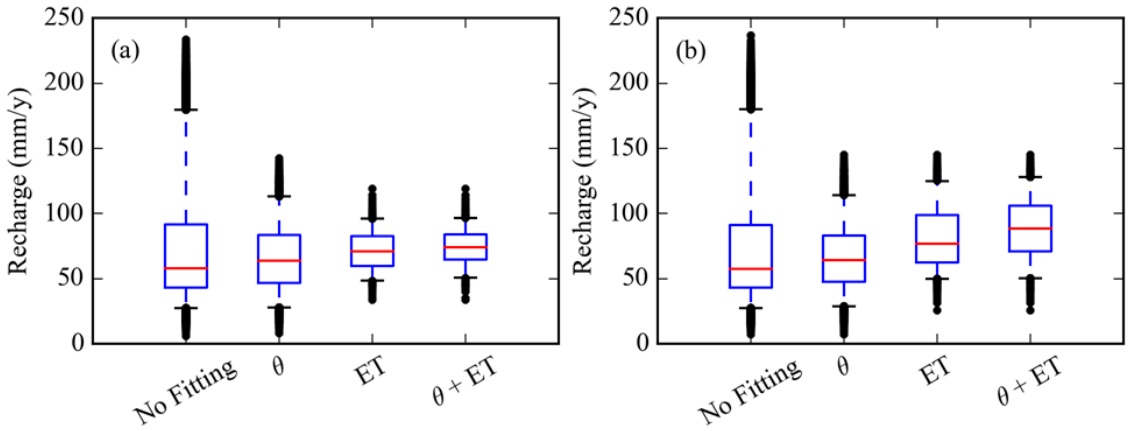

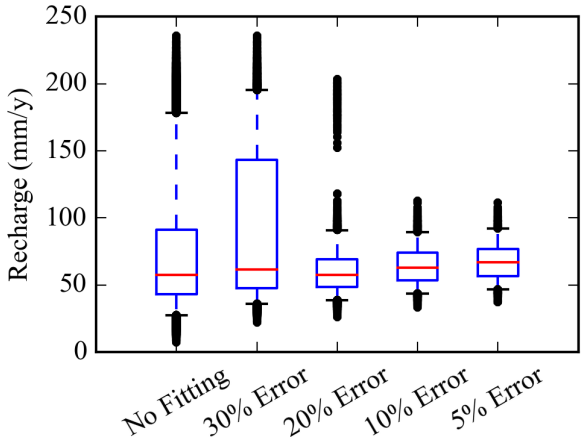

Table 1.

Function Type	Source	Soil Layer	K_s (m/d)	θ_s (cm^3/cm^3)	θ_r (cm^3/cm^3)	λ_c (m)	C (-)
Pedo1	Dane and Puckett (1992)	topsoil	0.138	0.263	0.15	0.206	10
		subsoil	0.00634	0.327	0.235	0.142	10
Pedo2	Saxton et al. (1986)	topsoil	0.257	0.377	0.0996	0.286	10
		subsoil	0.0583	0.417	0.176	0.227	10
Pedo3	Wösten et al. (1999)	topsoil	0.52	0.422	0.0788	0.487	10
		subsoil	0.169	0.421	0.128	0.296	10
Pedo4	Schaap et al. (2001)	topsoil	0.463	0.431	0.268	0.0347	10
		subsoil	0.189	0.428	0.306	0.0428	10

Table 2.

Parameter	Unit	Upper Bound	Lower Bound
1 minus albedo of the canopy, 1-α_c	—	0.9	0.8
1 minus albedo of the soil, 1-α_s	—	0.9	0.8
Rainfall interception coefficient *, K_r	m d^{-1} LAI^{-1}	0.002	0.0006
Light extinction coefficient *, k	—	-0.35	-0.65
Maximum carbon simulation rate, A_{max}	kg C m^{-2} d^{-1}	0.04	0.01
Slope parameter for the conductance model, g_1	—	1	0.8
Maximum plant available soil water potential, Ψ_{wilt}	m	-100	-200
IRM weighting of water, w_w	—	2.5	1.5
IRM weighting of nutrients, w_N	—	1	0.2
Ratio of stomatal to mesophyll conductance, *smc*	—	0.2	0.2
Temperature when the growth is 1/2 of optimum *, T_{half}	ºC	9	5
Temperature when the growth is optimum *, T_{opt}	ºC	19	15
Year day of germination, Day_g	d	100	150
Degree-daylight hours for growth, *DL*	ºC hr	20000	12000
Saturation light intensity *, L_{sat}	µmoles m^{-2} d^{-1}	1500	600
Maximum rooting depth, z_{max}	m	1.5	0.5
Specific leaf area, *SLA*	LAI kg C^{-1}	30	20
Leaf respiration coefficient, L_{rate}	kg C kg C^{-1}	0.002	0.0005
Stem respiration coefficient, S_{rate}	kg C kg C^{-1}	-1	-1
Root respiration coefficient, R_{rate}	kg C kg C^{-1}	0.0005	0.0001
Leaf mortality rate, M_{rate}	fraction of C d^{-1}	0.01	0.0001
Above-ground partitioning factor, β	—	0.6	0.3
Salt sensitivity factor, η	—	10	0.5
Aerodynamic resistance, r_a	s d^{-1}	40	20
Crop harvest index, *HI*	—	0	0
Crop harvest factor, *HF*	—	0	0

Table 3.

Test Case	θ			ET			θ + ET		
	N	90% (mm/y)	100% (mm/y)	N	90% (mm/y)	100% (mm/y)	N	90% (mm/y)	100% (mm/y)
1	9,999	28-114	7-144	2,107	44-90	33-113	1,543	47-92	33-113
2	10,000	28-113	8-142	1,172	48-96	33-119	992	51-97	34-119
3	9,998	29-114	7-145	2,589	50-125	26-145	1,875	50-128	26-145

Parameter uncertainty causes high uncertainty in groundwater recharge.

Evapotranspiration data can reduce recharge uncertainty by more than 50%.

Soil moisture data only reduce recharge uncertainty minimally compared to ET.

Recharge uncertainty reduces steadily as observation accuracy improves.